proceedings

MDPI

Proceedings

A New Chapter in Hard X-rays of the M87 AGN †

Ka-Wah Wong [1,*], Rodrigo S. Nemmen [2], Jimmy A. Irwin [3] and Dacheng Lin [4]

1 Eureka Scientific, Inc., 2452 Delmer Street Suite 100, Oakland, CA 94602-3017, USA
2 Universidade de São Paulo, Instituto de Astronomia, Geofísica e Ciências Atmosféricas, São Paulo, SP 05508-090, Brazil; rodrigo.nemmen@iag.usp.br
3 Department of Physics and Astronomy, University of Alabama, Box 870324, Tuscaloosa, AL 35487, USA; jairwin@ua.edu
4 Space Science Center, University of New Hampshire, Durham, NH 03824, USA; dacheng@dachenglin.com
* Correspondence: kw6k@virginia.edu
† Presented at the meeting Recent Progress in Relativistic Astrophysics, Shanghai, China, 6–8 May 2019.

Published: 30 September 2019

Abstract: The nearby M87 hosts an exceptional relativistic jet. It has been regularly monitored in radio to TeV bands, but little has been done in hard X-rays $\gtrsim$10 keV. For the first time, we have successfully detected hard X-rays up to 40 keV from its X-ray core with joint *Chandra* and *NuSTAR* observations, providing important insights to the X-ray origins: from the unresolved jet or the accretion flow. We found that the hard X-ray emission is significantly lower than that predicted by synchrotron self-Compton models introduced to explain very-high-energy γ-ray emission above a GeV. We discuss recent models to understand these high energy emission processes.

Keywords: accretion; accretion disks; black hole physics; galaxies: elliptical and lenticular; cD; galaxies: individual (M87); galaxies: nuclei; X-rays: galaxies

1. Introduction

Studying active galactic nuclei (AGNs) and their relativistic outflows or jets remains one of the most active areas of research in astrophysics today, both for probing black hole relativistic effects and because of their impact on the environment of the AGNs. Some of these AGNs are very-high-energy (VHE) TeV sources, suggesting that particles are accelerated to the same energy scale. Thus, studying these TeV emitting AGNs also provides important insights to the VHE radiative and accelerating mechanisms, which have a wide implication on other energetic phenomena.

One of the most famous AGNs is located at the center of the nearby radio galaxy M87 [1–3], whose jet was the first extragalactic one to be discovered [4]. Because of its proximity (D = 16 Mpc, 1 arcsec = 78 pc; [5]), the arcsecond-scale relativistic jet near the nucleus region can be resolved with radio ($\sim$40 micro-arcsecond: 230 GHz high frequency VLBI; [6]), optical (0.1 arcsec: *HST*), and X-ray (sub-arcsecond: *Chandra*) observations. Very recently, the central radio source has been successfully resolved down to its event horizon scale ($\sim$20 micro-arcsecond: [3]), and the resolved image is consistent with the black hole shadow predicted by general relativity.

The M87 galaxy is also a VHE ($>$100 GeV) source detected with *Fermi*, H.E.S.S., VERITAS, and MAGIC γ-ray telescopes [7]. It is one of the few radio galaxies with TeV γ-ray detected that are not strongly beamed sources [8,9]. Thus, studying M87 can provide a different scientific angle to understand the VHE particle acceleration mechanisms in AGNs (e.g., from a misaligned jet).

With multi-wavelength observations, the central region of M87 has already been resolved into different components at different angular scales: a central core where the supermassive black hole is located, a jet, and multiple knots along the jet direction (e.g., right panel in Figure 1 in X-ray). On the *Chandra* X-ray images, the most obvious features are the core and the bright knots (hereafter, we refer core as the central source unresolved by *Chandra* at sub-arcsecond scale). Outbursts have been seen from both the core and knots at different wavelength. Scientists in the community are not very sure about the precise locations of the highest energy bursts (GeV–TeV). It had been argued that the *HST*-1 knot outburst is responsible for the TeV outburst seen in 2005 (right panel in Figure 1; [10,11]). More recently, particularly with *Chandra* observations, support that the TeV emission originated from the unresolved *Chandra* core [7,12]. At this moment, the exact origin of the different energy emission is still under debate and is a very important research topic.

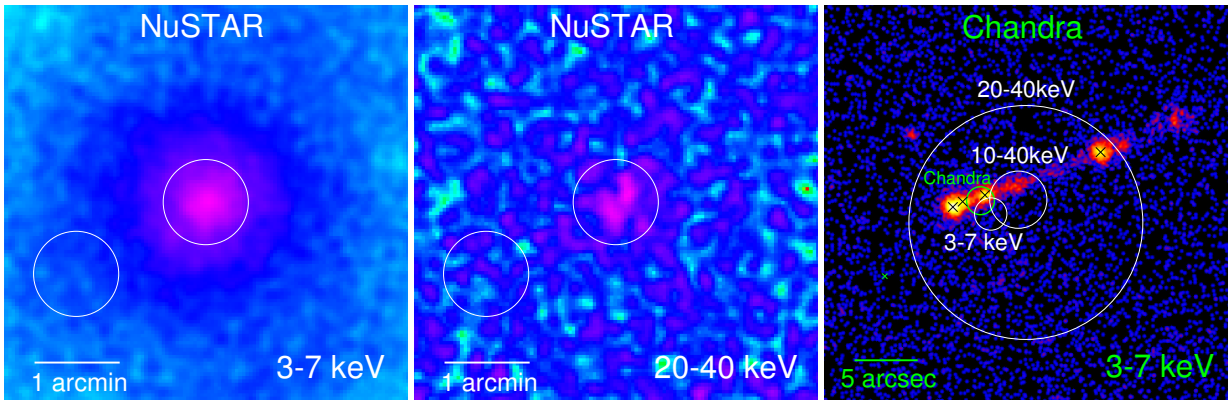

Figure 1. Smoothed *NuSTAR* images of M87 in the 3–7 keV (left) and 20–40 keV (middle) bands. The circles at the center and the lower left of the image indicate the spectral extraction regions of the source and the background, respectively. A high resolution *Chandra* image is shown in the right panel. The four crosses from the left to the right are the locations of the core, the *HST*-1 knot, knot D, and knot A, respectively. The three white solid circles indicate the 3σ position errors of the emission peaks measured with *NuSTAR* in different energy bands. Note that the green circle indicates the peak location of the *Chandra* image in the 3–7 keV band smoothed to the same spatial resolution as *NuSTAR* (FWHM = $18''$; smoothed *Chandra* image not shown). Although the *Chandra* core dominates the X-ray emission, the smoothed *Chandra* peak is shifted to the right from the core due to the X-ray contributions from the jet and the knots. Thus, the consistence of the peak positions in the soft and hard X-ray bands suggests that the spatial structure of the hard X-ray emission is consistent with that of the softer X-ray emission. These figures are modified from Wong et al. [13].

Distinguishing the precise location and the level of the emission is critical to understand the emission mechanism. Regardless of the uncertainties of the origin and models in explaining the full spectral energy distribution (SED), one thing is for sure: observations at all wavelengths are crucial to distinguish between various models. M87 is well monitored from radio to TeV energy. Spatial structures have been well resolved down to arcsec scale below the soft X-ray ($\sim$10 keV) band. The energy band beyond $\sim$10 keV, particularly the origin of hard X-rays was very uncertain due to the poor spatial resolution and sensitivity of the hard X-ray detectors. The first detection of hard X-ray emission (20–60 keV) from the M87 galaxy was reported by de Jong et al. [14] observed with *Suzaku*. With the poor spatial resolution of *Suzaku*, the exact location of the hard X-rays could not be determined, but it has been argued that the emission came from *HST*-1 mostly. It was still not clear how much (if any) hard X-ray emission can be produced by the core. With *simultaneous NuSTAR* and *Chandra* observations, we have detected, for the first time, hard

X-ray emission up to 40 keV from the M87 X-ray core, presumably in its quiescent state (Figure 1). In this paper, we summarize the key results of the observations and implications to recent theoretical models to explain the emission from the core.

2. Key Results

M87 was observed with *NuSTAR* on 2017 February 15, April 11, and April 14 (ObsIDs: 60201016002, 90202052002, and 90202052004). Four *Chandra* observations were taken during the three *NuSTAR* observations on 2017 February 15, February 16, April 11, April 14 (ObsIDs: 19457, 19458, 20034, and 20035). The details of the observations and data analysis were presented in Wong et al. [13]. Here, we summarize the key results of the observations.

2.1. X-ray Images

The left and middle panels of Figure 1 show the *NuSTAR* images in 3–7 keV and 20–40 keV, respectively. Hard X-ray emission in 20–40 keV is clearly detected at 7σ. The soft X-ray emission is extended, due to the strong intracluster medium (ICM) emission. The hard X-ray emission is not resolved, with its radial profile consistent with the $18''$ full width at half maximum (FWHM) of the *NuSTAR* point spread function (PSF).

Although the hard X-ray emission cannot be spatially resolved, the locations of soft and hard X-ray peaks can provide useful insight to the spatial structure of the hard X-ray emission. The right panel of Figure 1 shows that the peak location of the 10–40 keV hard X-ray emission is marginally consistent with the softer 3–7 keV peak. This suggests that the spatial structures of the soft and hard X-ray are consistent (i.e., core/knots/jet emission contaminated by ICM). To further support that the hard X-ray emission resembles the softer emission, we have smoothed the high resolution *Chandra* 3–7 keV image to match the spatial resolution of *NuSTAR*. The location of the smoothed *Chandra* peak is again consistent with that of the hard *NuSTAR* peak. We conclude that the origin of the hard X-ray emission above 10 keV is consistent with the origin of the softer emission.

2.2. X-ray Spectra

Although *NuSTAR* alone cannot spatially resolve the core, knots, and jet emission, we can make use of *Chandra* to spatially resolve and constrain these components and get a handle on the hard X-ray emission by joint fitting the spectra. All of these three components can be fitted by power-law models. Figure 2 shows the spectral components of the core (magenta; upper power-law), jet (orange; middle power-law), and *HST*-1 (cyna; lower power-law). The best-fit model parameters are summarized in Table 1.

Table 1. Best-fit spectral model parameters [13]. The power-law model of the photon flux is defined as $N(E) = KE^{-\Gamma}$, where E is the energy in keV, Γ is the photon index, and K is the normalization in units of 10^{-5} photons keV^{-1} cm^{-2} s^{-1} at 1 keV. Here, the flux $f = \int ENdE$ is in units of 10^{-13} erg cm^{-2} s^{-1}. The Γ parameter of *HST*-1 cannot be constrained in the joint fit and is fixed to the value determined with *Chandra* alone.

Name	Γ	K	$f_{20-40\,\mathrm{keV}}$
Core + *HST*-1 + Jet	$2.12^{+0.12}_{-0.13}$	102^{+38}_{-29}	$7.7^{+1.1}_{-1.0}$
Core	$2.11^{+0.15}_{-0.11}$	63^{+28}_{-15}	$4.8^{+0.9}_{-1.0}$
HST-1	[1.94]	$5.5^{+1.0}_{-0.9}$	$0.7^{+0.1}_{-0.1}$
Jet	$2.36^{+0.16}_{-0.17}$	52^{+10}_{-10}	$1.8^{+0.9}_{-0.6}$

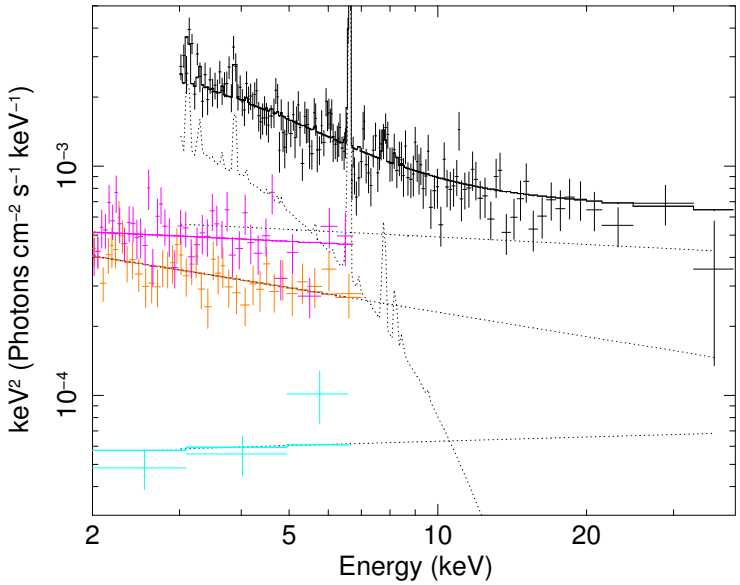

Figure 2. *NuSTAR* spectrum (black) joint-fitted with the *Chandra* spectra (color). The core (magenta; upper), jet (orange; middle), and *HST*-1 (cyan; lower) components joint-fitted to the *Chandra* spectra are shown. The three power-law, straight dotted lines are models for these three components best-fitted to the *NuSTAR* data. The dotted curve is the ICM component. The solid line is the total spectral model. This figure is reproduced from Wong et al. [13].

As *HST*-1 becomes fainter and fainter since its outburst in 2005, it does not dominate in X-ray anymore as observed in 2017. Instead, X-rays are dominated by the core emission. For the first time, hard X-ray emission is detected from its core.

3. Discussion

3.1. Jet or Accretion Flow?

The X-rays from the core are believed to come from either the advection-dominated accretion flow (ADAF) or the jet even unresolved with *Chandra* [15]. These two scenarios predict different spectral signatures, which in principle can be distinguished by spectral fitting.

Figure 3 shows the SED of the M87 core, the ADAF-dominated, and jet-dominated models of Nemmen et al. [15]. Both models were renormalized at X-ray. With *NuSTAR* data extending to 40 keV, it is quite clear that the X-ray emission above 1 keV is more consistent with the jet-dominated model. Note that the featureless jet emission probably cannot explain the entire SED, particularly the IR to UV bump. For example, the IR to UV emission might be ADAF-dominated and the X-rays might be jet-dominated, or the contributions of the two models can be more complicated. A global fitting by varying the parameters of both the ADAF and jet components instead of simply renormalizing the models is needed to correctly address the problem.

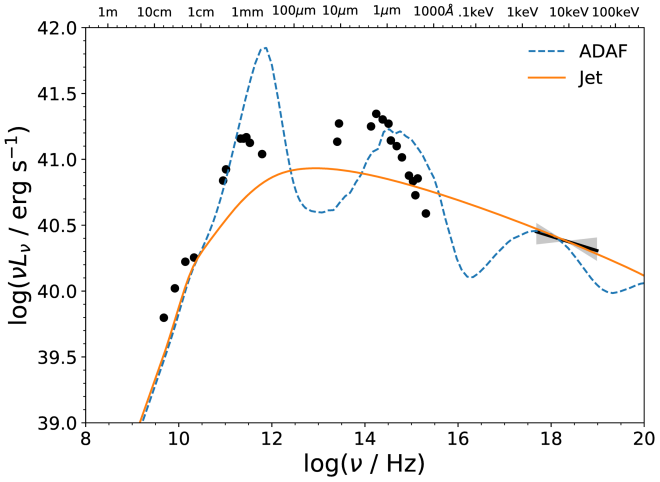

Figure 3. SED of the M87 core with X-ray data taken from Wong et al. [13] (grey: 90% confidence region in photon index) and the rest taken from the 0.″4 quiescent data of Prieto et al. [16]. The ADAF and jet models were renormalized to match in X-rays. These figure is reproduced from Wong et al. [13].

We also do not see any cut-off in the power-law spectrum in the X-ray range, which would be a signature of inverse-Compton scattering of photons from the hot corona of the accretion flow. Thus, we argue that the X-ray spectrum is more consistent with a jet origin, although emission from the ADAF cannot be completely ruled out. It is interesting that in another nearby radio galaxy, 3C 84, no cut-off in the power-law spectrum was found, and the hard X-ray emission is also more consistent with a jet origin [17]. The jet origin of the M87 core is also supported by Faraday rotation measure observations [18,19]. A more detailed discussion can be found in Wong et al. [13].

3.2. VHE Emission Mechanism?

On the higher energy end, in order to explain γ-ray and TeV emission from M87, the SED has been modeled using the one-zone synchrotron self-Compton (SSC) model that fits the softer X-ray ($\lesssim$10 keV) and above γ-ray emission fairly well during the quiescent state of the core (Figure 3 in de Jong et al. [14]; also, Figure 4 in Abdo et al. [20]). However, we found that they overpredict the hard X-ray emission at $\sim$40 keV by a factor of about three. Thus, the inverse Compton hump should be rising at an energy higher than $\sim$40 keV. It has been argued that the γ-ray emission above 10 GeV is associated with an additional emission component beyond the standard one-zone SSC model [21]. However, a recent study with multi-zone modeling also failed to reproduce the SED up to γ-ray scale [22], calling for further improvement of the theoretical modeling to understand the VHE emission process.

Author Contributions: K.-W.W. proposed the idea and methodology and carried out the formal analysis. All authors contributed to the investigation

Funding: This work was supported by NASA *Chandra* grants GO7-18085X and DD8-19098X and NASA *NuSTAR* grants NNX17GF12P and 80NSSC17K0634.

Conflicts of Interest: The authors declare no conflict of interest.

References

1. Macchetto, F.; Marconi, A.; Axon, D. J.; Capetti, A.; Sparks, W.; Crane, P. The Supermassive Black Hole of M87 and the Kinematics of Its Associated Gaseous Disk. *Astrophys. J.* **1997**, *489*, 579–600.

2. Gebhardt, K.; Thomas, J. The Black Hole Mass, Stellar Mass-to-Light Ratio, and Dark Halo in M87. *Astrophys. J.* **2009**, *700*, 1690–1701.
3. Event Horizon Telescope Collaboration. First M87 Event Horizon Telescope Results. I. The Shadow of the Supermassive Black Hole. *Astrophys. J. Lett.* **2019**, *875*, L1.
4. Curtis, H.D. Descriptions of 762 Nebulae and Clusters Photographed with the Crossley Reflector. *Pub. Lick Obs.* **1918**, *13*, 31.
5. Tonry, J.L.; Dressler, A.; Blakeslee, J.P.; Ajhar, E.A.; Fletcher, A.B.; Luppino, G.A.; Metzger, M.R.; Moore, C.B. The SBF Survey of Galaxy Distances. IV. SBF Magnitudes, Colors, and Distances. *Astrophys. J.* **2001**, *546*, 681–693.
6. Doeleman, S.S.; Fish, V.L.; Schenck, D.E.; Beaudoin, C.; Blundell, R.; Bower, G.C.; Broderick, A.E.; Chamberlin, R.; Freund, R.; Friberg, P.; et al. Jet-Launching Structure Resolved Near the Supermassive Black Hole in M87. *Science* **2012**, *338*, 355.
7. Abramowski, A.; Acero, F.; Aharonian, F.; Akhperjanian, A.G.; Anton, G.; Balzer, A.; Barnacka, A.; Barres de Almeida, U.; Becherini, Y.; Becker, J.; et al. The 2010 Very High Energy γ-Ray Flare and 10 Years of Multi-wavelength Observations of M87. *Astrophys. J.* **2012**, *746*, 151.
8. Rieger, F.; Levinson, A. Radio Galaxies at VHE Energies. *Galaxies* **2018**, *6*, 4.
9. Rani, B. Radio Galaxies-The TeV Challenge. *Galaxies* **2019**, *7*, 1.
10. Stawarz, Ł.; Aharonian, F.; Kataoka, J.; Ostrowski, M.; Siemiginowska, A.; Sikora, M. Dynamics and high-energy emission of the flaring HST-1 knot in the M 87 jet. *Mon. Not. R. Astron. Soc.* **2006**, *370*, 981–992.
11. Cheung, C.C.; Harris, D.E.; Stawarz, Ł. Superluminal Radio Features in the M87 Jet and the Site of Flaring TeV Gamma-Ray Emission. *Astrophys. J. Lett.* **2007**, *663*, L65.
12. Aharonian, F.; Akhperjanian, A.G.; Bazer-Bachi, A.R.; Beilicke, M.; Benbow, W.; Berge, D.; Bernlöhr, K. Fast Variability of Tera-Electron Volt γ Rays from the Radio Galaxy M87. *Science* **2006**, *314*, 1424–1427.
13. Wong, K.-W.; Nemmen, R.S.; Irwin, J.A.; Lin, D. Hard X-Ray Emission from the M87 AGN Detected with NuSTAR. *Astrophys. J. Lett.* **2017**, *849*, L17.
14. De Jong, S.; Beckmann, V.; Soldi, S.; Tramacere, A.; Gros, A. High-energy emission processes in M87. *Mon. Not. R. Astron. Soc.* **2015**, *450*, 4333–4341.
15. Nemmen, R.S.; Storchi-Bergmann, T.; Eracleous, M. Spectral models for low-luminosity active galactic nuclei in LINERs: the role of advection-dominated accretion and jets. *Mon. Not. R. Astron. Soc.* **2014**, *438*, 2804–2827.
16. Prieto, M.A.; Fernández-Ontiveros, J.A.; Markoff, S.; Espada, D.; González-Martín, O. The Central Parsecs of M87: Jet Emission and an Elusive Accretion Disc. *Mon. Not. R. Astron. Soc.* **2016**, *457*, 3801–3816.
17. Rani, B.; Madejski, G.M.; Mushotzky, R.F.; Reynolds, C.; Hodgson, J.A. NuSTAR View of the Central Region of the Perseus Cluster. *Astrophys. J. Lett.* **2018**, *866*, L13.
18. Feng, J.; Wu, Q.; Lu, R.-S. An Accretion-jet Model for M87: Interpreting the Spectral Energy Distribution and Faraday Rotation Measure. *Astrophys. J.* **2016**, *830*, 6.
19. Li, Y.-P.; Yuan, F.; Xie, F.-G. Exploring the Accretion Model of M87 and 3C 84 with the Faraday Rotation Measure Observations. *Astrophys. J.* **2016**, *830*, 78.
20. Abdo, A.A.; Ackermann, M.; Ajello, M.; Atwood, W.B.; Axelsson, M.; Baldini, L.; Ballet, J.; Barbiellini, G.; Bastieri, D.; Bechtol, K.; et al. Fermi Large Area Telescope Gamma-Ray Detection of the Radio Galaxy M87. *Astrophys. J.* **2009**, *707*, 55–60.
21. Ait Benkhali, F.; Chakraborty, N.; Rieger, F.M. Complex Gamma-ray Behavior of the Radio Galaxy M 87. *Astron. Astrophys.* **2019**, *623*, A2.
22. Lucchini, M.; Krauß, F.; Markoff, S. The unique case of the AGN core of M87: a misaligned low power blazar? *Mon. Not. R. Astron. Soc.* **2019**, *489*, 1633–1643.

© 2019 by the authors. Licensee MDPI, Basel, Switzerland. This article is an open access article distributed under the terms and conditions of the Creative Commons Attribution (CC BY) license (http://creativecommons.org/licenses/by/4.0/).